Real-time kinetic studies of *Mycobacterium tuberculosis* LexA-DNA interaction

Chitral Chatterjee[1], Soneya Majumdar[1], Sachin Deshpande[1], Deepak Pant[1],

Saravanan Matheshwaran*[1, 2]

[1]Department of Biological Sciences and Bioengineering, Indian Institute of Technology, Kanpur, U.P.

[2]Centre for Environmental Sciences and Engineering, Indian Institute of Technology Kanpur, U.P.

*To whom correspondence should be addressed: Saravanan Matheshwaran, Phone: +91-512-259-4066; Fax: +91-512-259-4010; E-mail: saran@iitk.ac.in

Keywords

"SOS" response, LexA, *Mycobacterium tuberculosis*, Transcriptional repressor, Bio-layer Interferometry, DNA binding

Running title: Real-time kinetic analysis of Mtb LexA-DNA interaction

Abstract

Transcriptional repressor, LexA, regulates the "SOS" response, an indispensable bacterial DNA damage repair machinery. Compared to its *E.coli* ortholog, LexA from *Mycobacterium tuberculosis* (Mtb) possesses a unique N-terminal extension of additional 24 amino acids in its DNA binding domain (DBD) and 18 amino acids insertion at its hinge region that connects the DBD to the C-terminal dimerization/autoproteolysis domain. Despite the importance of LexA in "SOS" regulation, Mtb LexA remains poorly characterized and the functional importance of its additional amino acids remained elusive. In addition, the lack of data on kinetic parameters of Mtb LexA-DNA interaction prompted us to perform kinetic analyses of Mtb LexA and its deletion variants using Bio-layer Interferometry (BLI). Mtb LexA is seen to bind to different "SOS" boxes, DNA sequences present in the operator regions of damage-inducible genes, with comparable nanomolar affinity. Deletion of 18 amino acids from the linker region is found to affect DNA binding unlike the deletion of the N-terminal stretch of extra 24 amino acids. The conserved RKG motif has been found to be critical for DNA binding. Overall, this study provides insights into the kinetics of the interaction between Mtb LexA and its target "SOS" boxes. The kinetic parameters obtained for DNA binding of Mtb LexA would be instrumental to clearly understand the mechanism of "SOS" regulation and activation in Mtb.

Introduction

The expression of DNA damage and stress response genes, which serve to preserve genome integrity upon exposure to DNA damaging agents, is controlled by the "SOS" response pathway. Activation of the "SOS" response helps the bacteria to develop resistance to antibiotics, making it indispensable for survival and growth under adverse conditions (1-3). This pathway is regulated by two key players, namely, RecA and LexA. LexA binds to a consensus sequence of DNA known as the "SOS" box located in the operator region of several genes and transcriptionally represses them under normal physiological conditions. However, under stress conditions, LexA falls off from the operators leading to activation of these genes to facilitate DNA repair (4). The "SOS" regulons exhibit significant variations across the bacterial kingdom, reflecting their overall complexity. For example, while *Bacillus subtilis* harbors only 33 genes in its "SOS" regulon, *E.coli* contains over 45 genes (5). Most of the "SOS" regulons include genes that encode for error-prone DNA polymerases, LexA, RecA, and proteins involved in the nucleotide excision repair pathway, although exceptions are known to exist (6).

"SOS" activation occurs in the following sequence of events— (i) RecA interacts with single-stranded DNA to form activated nucleoprotein filament complex, (ii) activated RecA directly interacts with LexA leading to autoproteolytic cleavage of the latter, and finally (iii) LexA falls off from the operator regions causing transcriptional de-repression of the damage-inducible genes (7). In *E.coli,* the LexA repressor binds to consensus "SOS" box sequence present in different operators, with variable affinity (7). Genes with lower operator-repressor affinity are activated early on in the "SOS" pathway when compared to genes having tightly bound operators. For instance, genes such as *lexA, uvrA, uvrB, uvrD, and recA* express early on, while those encoding for error-prone polymerases, (*dnaE2, umuD)* and

63 *sulA* express much later in the cascade (7). Altogether, the differential binding of LexA to
64 different operators results in a highly complex but well-coordinated process that protects the
65 cellular machinery during DNA damage.

66 LexA homologs are widespread across bacterial genomes and have remained
67 evolutionarily conserved (8). While most of the DNA damage-inducible genes in *E.coli* are
68 under the direct control of LexA/RecA, such is not in the case of
69 *Mycobacterium tuberculosis* (Mtb), wherein several DNA damage-inducible genes are
70 independent of LexA regulation (9). Among the 21 genes regulated by LexA/RecA in Mtb,
71 only a few have been characterized, limiting our present understanding of the molecular
72 mechanisms underlying the regulatory role of LexA. The functional characterization of
73 LexA, including estimation of kinetic parameters obtained from binding to different "SOS"
74 boxes, will provide new insights in mechanistically understanding mycobacterial "SOS"
75 regulation.

76 Well-studied LexA homologs from *E.coli* and *B.subtilis* are known to exhibit
77 nanomolar binding affinities towards "SOS" box DNA with an apparent K_D of 0.8 nM and
78 2.3 nM respectively (10, 11). However, a lack of kinetic analyses for Mtb LexA-DNA
79 interaction greatly limits our understanding of mycobacterial "SOS" activation. Nearly 25 *in-*
80 binding sites of LexA were identified in the Mtb genome by Davis and colleagues in 2012
81 (12). The study demonstrates differential expression of the damage-inducible genes upon
82 Mitomycin C-induced stress (12). Precise quantitation of such molecular interactions of Mtb
83 LexA with DNA could reveal the importance of structural integrity and the mechanism of
84 "SOS" induction. To address this, it is imperative to study the kinetics of the interaction of
85 LexA with its target binding sites and thus we carried out real-time Mtb LexA-DNA
86 interaction studies.

Although the C-terminal domain (CTD) crystal structure of Mtb LexA provides a molecular framework for its architecture and assembly, the DNA binding domain (DBD) remained inaccessible for structural studies (13). Mtb LexA has an N-terminal DBD and a C-terminal dimerization/catalytic domain separated by a linker region similar to its orthologs from other bacteria. Notably, sequence comparison between Mtb and *E.coli* LexA revealed a unique N-terminal extension of 24 amino acids, which came into light after the re-annotation of Mtb LexA by Smollett *et al*., in 2009 (14), and a longer linker region with additional 18 amino acids in Mtb LexA. Further, the functional importance of these extra stretches of amino acids in and around the DBD and linker region of Mtb LexA remains unclear. Therefore, in this study, we investigated whether these unique regions play any role in DNA binding. We have generated Mtb LexA mutants that lack 24 amino acids from its N-terminal domain (NTD), 18 amino acids from its linker region, in addition to mutating the conserved DNA binding residues "RKG" to "AAA". We have compared the DNA binding property of these mutants with wild-type Mtb LexA qualitatively using EMSA and quantitatively by Bio-layer Interferometry (BLI) to obtain real-time binding kinetic parameters. The DNA binding assessed using BLI revealed a comparable binding affinity of wild-type Mtb LexA and its N-terminal 24 amino acids truncation variant. Deletion of 18-amino acids from the linker resulted in 16 times reduced binding, whereas RKG mutant showed no binding, suggesting their importance in DNA binding. The kinetic parameters of Mtb LexA-DNA interaction obtained from this study provide new functional insights crucial for an understanding of mycobacterial "SOS" regulation.

Materials and Methods

Plasmids, strains, and reagents

Bacterial strains and plasmids used in the study are listed in **Table S1** of **Supplementary Material**. Primers and oligonucleotides were purchased from Sigma Aldrich and are listed along with the constructs generated in the study in **Table S2** of **Supplementary Material**. All the reagents, media, and chemicals were purchased from Sigma Aldrich, Hi-Media, and SRL, and enzymes were purchased from New England Biolabs.

Construction and analysis of phylogenetic tree

Multiple sequence alignment of LexA proteins from diverse bacterial groups was created using Clustal X and the phylogenetic tree was constructed using RaxML (15). The evolutionary history of the taxa has been inferred from 1000 replicates of the bootstrap consensus tree. The percentage of replicates in which clustering of related taxa took place is mentioned next to the branches. 283 positions were found in the final dataset. iTOL was used to visualize the generated tree (16).

Over-expression and purification of proteins

The Mtb LexA and its Δ24aa variant were individually cloned between NdeI and BamHI restriction sites, respectively in pET28a(+) bearing N-terminal 6x His tag. Mtb LexAΔ18aa and Mtb LexA RKG/AAA mutants were generated by the overlap PCR method. The primers used have been listed in **Table S2** of **Supplementary Material**. All constructs generated have been confirmed by sequencing.

The recombinant WT and its variant proteins were over-expressed in *E.coli* BL21 (DE3) cells. Cultures were induced with 0.5 mM IPTG at $O.D_{600}$ 0.6. The cells were pelleted

after 4 hrs by centrifugation at 5000×g following which the pellet was resuspended in Lysis Buffer composed of 50 mM Tris-Cl (pH 8.0), 150 mM NaCl and 10 mM imidazole (pH 8.0), 5% glycerol, 1mM Phenylmethylsulfonyl fluoride (PMSF). After lysing the cells by sonication on ice (10" On, 30" Off cycles), the clarified lysate was centrifuged for 1h at 20,000g. The clarified supernatant was passed through a pre-equilibrated HisTrap HP column at 5ml/min. Column was washed with 50 mM Tris-Cl , 500 mM NaCl, 30 mM imidazole (pH 8.0) and proteins were subsequently eluted under a gradient in 25 mM Tris-Cl (pH 8.0), 150 mM NaCl and 750 mM imidazole (pH 8.0). Pure fractions were pooled, diluted with a low salt buffer (25 mM Tris-Cl (pH 8), 100 mM NaCl, 1 mM EDTA, 5% glycerol), and loaded onto Q-Sepharose column for anion exchange chromatography. Proteins were eluted in gradient by passing a high salt buffer (25 mM Tris-Cl (pH 8.0), 1 M NaCl, and 1 mM EDTA). The pure fractions were concentrated using Gel Filtration Buffer (20 mM Tris-Cl (pH 8.0), 100 mM NaCl and 5% glycerol) and separated using Superdex 75 10/300 GL for gel filtration. The purified proteins were run on 12% SDS-PAGE for analyzing their purity and concentrations were determined via spectrophotometric analysis.

Cross-linking reactions

The cross-linking reactions were performed by incubation of each of the proteins at 5 μM final concentration in presence of 0.01% v/v glutaraldehyde in 10 mM HEPES (pH 8.0), 50 mM NaCl for 30 mins on ice. The reactions were stopped with 25 mM of DTT. Samples were separated on a 12% SDS-PAGE.

Circular dichroism (CD)

CD spectra were recorded from 195-280 nm using a Jasco J-815 spectropolarimeter. A 1 mm pathlength quartz cuvette was used. Resolution up to 0.2 nm was maintained with a scan rate

of 100 nm/min. 25°C was maintained for all experiments. 5 μM of each protein in 10 mM Tris-Cl 50 mM NaCl (pH 7.5) was taken for analysis. The data presented is an average of three scans after correction for the buffer baseline. Recorded spectra were analyzed using Origin 8.1 software.

Extrinsic Fluorescence

Extrinsic fluorescence spectra were obtained using a Jobin-Yvon Fluorometer FluoroMax3, at 25°C. 5 μM of each of the proteins in 10 mM Tris-Cl (pH 7.5), 50 mM NaCl were incubated with 44 mer ds *dnaE2* "SOS" box containing DNA (sequence given in **Table 1**) at 1:2 ratio for 30 mins at 37°C. The samples were incubated with 40 μM of ANS in dark for 10 mins. Samples were excited at 350 nm, and in the range of 400 to 600 nm, emission spectra were recorded. Measurements were corrected for fluorescence intensity of buffer, DNA, and ANS intrinsic fluorescence.

Electrophoretic mobility shift assay

WT and its variants at 128 nM were incubated in presence of 3.5 nM of end-labeled (non-biotinylated) 44 mer ds *dnaE2* "SOS" box containing DNA (sequence given in **Table 1**) in 10 mM HEPES (pH 7.5), 50 mM NaCl for 30 mins on ice. The unbound DNA and DNA-protein complexes were resolved on 8% native PAGE at 100V for 1 h in cold. Gels were dried and autoradiographed. The same procedure was followed for EMSA analysis in which increasing concentrations (0-128 nM) of WT Mtb LexA was incubated with ^{32}P end-labeled ds 44 mer ds *dnaE2* "SOS" box containing DNA.

Bio-layer Interferometry (BLI)

The ForteBio Octet RED 96 (Forte Bio, USA) platform was used to conduct interaction studies between LexA and its variants with biotinylated ds 44mer of different "SOS" boxes containing sequences (listed in **Table 1**). Streptavidin matrix-coated sensor chip (SA) was equilibrated in 10 mM HEPES (pH 7.5), 50 mM NaCl followed by immobilization of 100 nM of biotinylated ds DNA on it. Increasing concentrations of WT and mutant proteins were passed onto the chip and change in response units (RU) was analyzed. The program comprises one-minute stabilization of the baseline with the buffer followed by ten-minute loading of sensors with biotinylated DNA, a five-minute association enabling interaction between the protein and DNA, a five-minute dissociation step finally followed by a five-second regeneration step (unless mentioned otherwise). A reference sensor dipped in the buffer was used as a background control. All analyses were carried out at 25°C. A 1:1 binding model was applied to globally fit the binding isotherms and kinetic parameters such as k_{on}, $k_{off,}$ and K_D were obtained. The experiments were performed in triplicates.

Results and Discussion

Mtb LexA features distinct characteristics from its counterparts

LexA is present in most bacterial species and phyla (17). Evolutionarily, the protein has retained its two distinct domains, the NTD, involved in DNA binding, and CTD, which is responsible for dimerization and autoproteolytic cleavage. Alpha helices involved in DNA binding and the residues critical for autoproteolysis have remained well conserved across different species, thereby preserving the overall functions of the protein.

From an evolutionary viewpoint, a comparison between LexA homologs from selected representatives belonging to major classes of Gram-positive, Gram-negative, Archaebacterial, and Actinobacterial phyla reveals the discrete clustering based on their classification, evident from the phylogenetic tree constructed (**Figure 1A**). This tree has been deduced by comparing sequences from 24 representative bacterial species (shown in **Figure S1** of **Supplementary Material)**. LexA homologs from Actinobacteria closely resemble homologs from Gram-positive Firmicutes which is consistent with their relatedness at the species level. Interestingly, LexA from members of Actinobacteria that include the pathogenic tuberculous mycobacteria such as Mtb, *M.canetti, M.bovis,* shows significant similarity, suggesting a possible link between pathogenicity and sequence evolution of LexA.

Subsequent comparison of the LexA sequences among some of the well-known tuberculous and non-tuberculous mycobacteria revealed interesting results. Although the C-terminal regions remain almost identical, N-terminal regions exhibit sequence variations especially at the terminal end. Pathogenic mycobacteria have relatively smaller genome sizes (18) and are not expected to code for unwanted additional stretches of amino acids in their proteins unless they prove advantageous for their survival. Interestingly, tuberculous mycobacteria except for *M.bovis* were found to possess additional amino acids at the N-terminal end of LexA, unlike their *E.coli* counterpart, implying unexplored adaptive functions. Another region of less conservation spans the linker region that connects the NTD and CTD of the protein. While the latter half of the linker sequences (towards the CTD) exhibits more conservation, the initial half varies among different mycobacterial species. Although the linker is identical between Mtb and *M.bovis* harboring 25 amino acids, the number of residues and sequence conservation vary among the other mycobacteria (**Figure 1B**). In *M.leprae* and *M.haemophilum,* the linker can extend up to 28 amino acids long. LexA

possessing additional stretches of amino acids triggers the curiosity to explore their mechanistic roles in “SOS” induction that could help mycobacterial survival and evolution.

Presumably, these stretches of amino acids in Mtb LexA that remain uncharacterized may confer additional functions unique to mycobacterial species when compared to its well-characterized homologs. LexA is a global repressor controlling the expression of DNA repair genes. Hence, assessing whether these additional stretches of amino acids may influence interactions with “SOS” boxes could provide new information related to “SOS” regulation. Considering both the additional stretches of amino acids to lie in proximity to the DNA binding regions of the protein, we deleted these stretches to explore their impact on DNA binding. Subsequently, the stretch of 24 amino acids (residues 1-24) was deleted to generate LexAΔ24aa and LexAΔ18aa was generated by deleting 18 amino acids spanning the hinge region (residues 94-111) of the protein. This long hinge region separates the NTD from its CTD in Mtb LexA. This is in sharp contrast to the much shorter hinge region of just 4 amino acids (Q70-E74) present in *E.coli* (**Figure 1B**). The functional relevance of such a long hinge region in Mtb has not been explained. Possibly, the longer length of this inter-domain linker in Mtb LexA can enhance its flexibility to attain suitable conformations for binding to DNA (13). Next, we have attempted to shed light on this aspect in the present study by characterizing and comparing the DNA binding ability of the variants with that of WT LexA. RKG motif involved in DNA binding contains Arg 52, Lys 53, and Gly 54 in *E.coli* LexA lying in the third alpha helix of the protein, (19) and its corresponding Arg 75, Lys 76 and Gly 77 residues of Mtb LexA have remained conserved. We have mutated these residues to assess whether they are essential for DNA binding in Mtb LexA.

Evaluation of Mtb LexA and its variants for dimerization and DNA binding property

All proteins were purified to ~98% purity (**Figure 1C**). Near and far UV spectra of Mtb LexA and its mutants were used to assess changes in their secondary structures due to mutations (**Figure 2A**). Interestingly, both far (195-250 nm) and near (250-280 nm) UV spectra from Circular Dichroism (CD) studies revealed the comparable secondary structures of WT Mtb LexA and its mutants.

All the variants predominantly exist as dimers in solution as analyzed from profiles of gel filtration chromatography (**Figure S2** of **Supplementary Material**). To confirm this further, the purified proteins were subjected to cross-linking using the chemical cross-linker glutaraldehyde. Upon cross-linking, the predominant form appeared to be dimeric in all cases as evident from the top band running between 48 and 63kDa (**Figure 2B**). Structural analysis of the C-terminal segment of Mtb LexA revealed residues 229-236 along with residues 139-153 from its NTD to be involved in dimer formation between two LexA monomers (13). The mutants generated in this study have no overlapping sequences with the afore-mentioned residues and therefore, all of them retained the ability to form dimers. Therefore, a comparable profile of results in CD spectroscopy and protein dimerization experiments revealed that the selected regions had minimal or no influence on the secondary structure of Mtb LexA.

Next, we used fluorescence spectroscopy to assess the structural changes of Mtb LexA and its variants upon interaction with DNA. Hydrophobic extrinsic fluorescent dye 8-anilino-1-naphthalenesulfonic acid (ANS) has been widely used for screening the alterations in the tertiary structure of proteins and to monitor their ligand-binding events such as protein-nucleic acid interactions (20). The ligand displaces the fluorescent dye upon binding to the protein, resulting in a quench in fluorescence. Changes in fluorescence intensity are a direct

readout of protein-DNA binding. The maximum quench in fluorescence intensity was noted when WT LexA formed a complex with DNA (**Figure 2C**). A similar quench in fluorescence intensity was observed for LexAΔ24aa and the WT protein upon DNA binding (**Figure 2F**), suggesting that the 24 amino acids extension is not crucial for DNA binding. However, we cannot overlook the possibility that it may have a regulatory role in DNA binding which could be dependent on the "SOS" box sequences (21). In striking contrast to LexAΔ24aa, deleting 18 amino acids from the linker region has significantly reduced the fluorescence quenching to nearly half compared to that for the WT, suggesting that this linker region may play a prominent role in DNA binding (**Figure 2E**). The deletion of 18-amino acids had weak or no effect on the secondary structures; however, the observed reduction in nucleic acid binding affinity may be influenced by the Van der Waals interactions offered by either glutamic acid or aspartic acid residues (4 out of 18 amino acid residues) within the linker region. Lastly, RKG/AAA mutant showed no significant fluorescence quench upon interaction with DNA (**Figure 2D**), thereby establishing that RKG residues play a critical role in DNA binding in Mtb LexA similar to the other orthologs. Further, we have carried out electrophoretic mobility shift assays (EMSA) to see the DNA binding of WT LexA to the *dnaE2* "SOS" box. The shift in the ^{32}P labelled *dnaE2* "SOS" box DNA suggests that Mtb LexA can bind to "SOS" box with nM affinity (**Figure 3A**). We have also performed EMSA with Mtb LexA variants. EMSA analysis revealed that LexAΔ24aa and LexAΔ18aa showed mobility shift, whereas RKG/AAA mutant did not show any DNA binding (**Figure 3B**). This further confirms the importance of the RKG motif in DNA binding. Based on these observations, we further decided to quantitate the real-time kinetic parameters of LexA-DNA interactions with WT LexA and its variants.

Determination of DNA binding kinetics of Mtb LexA and its variants

We used BLI for determining the DNA binding affinity for Mtb LexA and its mutants. First, we characterized the interaction between WT Mtb LexA and its variants to the perfectly palindromic *dnaE2* "SOS" box ("SOS" box sequence given in **Table 1)**. WT and its variant, LexAΔ24aa, exhibit comparable DNA binding affinity (K_D of 2.16±0.01 nM for WT and 4.94±0.03 nM for LexAΔ24aa, respectively). Further, LexAΔ24aa with and without N-terminal 6x His tag showed comparable DNA binding kinetics (**Figure S3**).

LexA18aaΔ variant shows significantly reduced affinity as seen from the sensograms depicted in **Figure 4**. Deleting 18 amino acids from the linker connecting NTD and CTD resulted in a more than fifteen times reduction in affinity when compared to the full-length protein, with an obtained K_D of 34.4±0.19 nM (**Table 2**). The rate of association (k_{on}) was highest in the order of 10^6 for full-length Mtb LexA and decreased to the order of 10^4 in the case of the Δ18aa variant. While the association rate constants varied, the dissociation rate constants (k_{off}) did not change significantly. We speculate that deleting the 18 amino acids from the linker affected the conformation to bind DNA suitably, thereby reducing its association rate (**Figure 4B, Table 2**). We did not observe any detectable binding for RKG/AAA, even after doubling the time of interaction (from 300 to 600 seconds of association) (**Figure 4G**), indicating the RKG motif in DBDs is critical for the DNA binding. Altogether, Mtb LexA exhibits similarity to *E.coli* counterpart in terms of binding to its cognate "SOS" box with nanomolar affinity. Additionally, the presence of the longer linker in Mtb LexA is found to positively affect its DNA binding ability. The kinetic parameters obtained by performing experiments at physiological pH intrigued us to investigate how they would vary when subjected to acidic conditions. The rationale behind choosing a highly acidic pH condition to monitor changes in DNA binding affinity of Mtb LexA arises from the

fact that Mtb is known to face a hostile environment of acidic pH inside host macrophages and is challenged to maintain internal pH homeostasis for survival (22). Although internal pH lower than 6 is noted to be lethal for mycobacteria, it has to endure external pH as low as 4 (22). We wanted to assess whether Mtb LexA and its variants could exhibit DNA binding even at an extreme pH such as pH 4.

We found that Mtb LexA exhibited maximal and optimal binding with the perfectly palindromic *dnaE2* "SOS" box near physiological pH (pH 7.5). Surprisingly, Mtb LexA retained the ability to bind DNA even at pH 4, although with reduced affinity (**Figure 5**). The dissociation constants changed from 2.16±0.01, 4.94±0.03 and 34.4±0.19 nM (at pH 7.5) to 75.99±0.27, 29.94±0.13 and 111±0.33 nM (at pH 4) for WT, LexAΔ24aa and LexAΔ18aa, respectively. Binding at acidic pH (pH 4) can thus be said to have reduced by nearly 35 times for the wild-type protein, nearly 6 times for LexAΔ24aa, and nearly 3.2 times for LexAΔ18aa when compared to physiological conditions (**Table 2**). From the kinetic parameters observed, we notice a significant reduction in association rate constants (k_{on}) at low pH (pH 4) compared to physiological conditions (pH 7.5) for wild-type protein and its Δ24aa variant while the change is not so pronounced in the case of the Δ18aa variant. Dissociation rate constants (k_{off}) in the case of WT Mtb LexA remained comparable in both the pH conditions tested but reduced by a power of 10 for the mutant proteins at low pH. Mutants seem to both associate and dissociate faster at physiological pH as compared to low pH and as for the wild-type protein, there has been a drastic reduction only in its rate of association to bind DNA at low pH conditions.

Our observations results corroborate with those made from *in-vitro* studies that have assessed the effect of variations in pH in regulating the "SOS" response for *E.coli* LexA (23-25). Relan and co-workers reported that *E.coli* LexA bound to its operator maximally near

344 physiological pH displaying about ten-fold better binding compared to that at pH 4 (23).
345 Similarly, we noticed a reduction in DNA binding by Mtb LexA as well, at acidic pH. It will
346 be interesting to decipher the molecular events leading to this.

347 **DNA binding kinetics of Mtb LexA with different "SOS" boxes**

348 The differential gene expression profile following DNA damage led to the identification of
349 genes that fall under direct regulation of LexA in Mtb (21). However, DNA binding kinetics
350 of LexA to "SOS" boxes of these DNA damage-inducible genes remained uncharacterized.
351 We, therefore, determined the DNA binding affinity for LexA and its mutants to different
352 mycobacterial "SOS" boxes (the kinetic parameters determined for the interaction of mutants
353 to different "SOS" boxes are provided in **Figure S4** and **Table S3** of **Supplementary**
354 **Material**). The "SOS" boxes chosen have unique characteristics (**Table 1**). While the *dnaE2*
355 "SOS" box is a perfect palindrome throughout (as mentioned in the previous section), *lexA*
356 and *recA* "SOS" boxes have one mismatch towards their 3'ends (on the flank). *rv3074* "SOS"
357 box is unique in displaying a perfect palindrome of sequences on either side repeat flanks but
358 showing mismatches in sequences between the flanks. All the genes whose "SOS" boxes
359 have been chosen for the present study are highly induced following DNA damage in Mtb
360 (21).

361 Increasing concentrations of WT LexA and its variants (analytes) were allowed to
362 interact with biotinylated "SOS" boxes till saturation in binding was achieved. WT LexA was
363 found to bind to different "SOS" boxes with close affinities (**Figure 6, Table 3**). K_D values
364 ranged from 0.98±0.01 nM for the *lexA* "SOS" box to 3.86±0.03 nM as noted for the *rv3074*
365 "SOS" box. The association rate was relatively higher for *dnaE2* and *lexA* "SOS" boxes as
366 compared to the other two "SOS" boxes. The perfectly palindromic nature of the dnaE2
367 "SOS" box facilitates faster association with LexA. *dnaE2* encodes an error-prone DNA

polymerase, hence its regulation must be strictly controlled. It is known that genes that are involved in mutagenesis such as these error-prone DNA polymerases are expressed later in the "SOS" response cascade and are tightly controlled (26). Our observation confirms the same in the case of Mtb.

Although the association rate constants (k_{on}) varied for different "SOS" boxes, the corresponding dissociation rate constants (k_{off}) are also seen to change proportionately; hence, the overall K_D is not widely altered for different "SOS" boxes tested here. Though, no drastic changes in binding affinity to different "SOS" boxes are noted here, studying these repressor-DNA binding events extensively in the cellular context can reveal additional modes of regulation or factors modulating the expression patterns of "SOS" responsive genes at the time of "SOS" activation.

Conclusion

Mtb LexA controls gene expression patterns of the crucial "SOS" response pathway that facilitates mycobacterial adaptation to stress (12). However, lack of thorough understanding at the molecular level, taking into account the unique regions of Mtb LexA that could potentially influence its interaction with DNA, prompted us to execute this study by analyzing the impact of such truncations/ mutations on Mtb LexA-DNA interaction. Together, we present our detailed analysis of Mtb LexA and the role of its additional stretches of amino acids in regulating the "SOS" response.

To begin with, the deletion and mutated variants displayed comparable secondary structure as that of wild-type Mtb LexA protein, inferred from the ellipticity measurements carried out using circular dichroism. Moreover, they retained the ability to form dimers as observed from size exclusion chromatography and crosslinking studies.

Qualitative estimation and comparative analysis of protein-nucleic acid interaction of the variants compared to the WT revealed that while the 24-amino acid extension at the N-terminal is not critical for Mtb LexA-DNA association, deletion of the 18 amino acids linker connecting the NTD and CTD of the protein resulted in a marked reduction in DNA binding compared to the full-length protein. The 18 amino acids present in the linker most likely accounts for the conformational flexibility of Mtb LexA to suitably bind DNA. Moreover, mutating the RKG motif in the DNA binding helix abolished LexA-DNA binding, highlighting the significance of strong evolutionary conservation of this motif across different organisms.

The quantitation of DNA binding in real-time has been carried out using BLI and kinetic parameters of Mtb LexA-DNA interaction have been determined. The binding affinity of WT Mtb LexA (K_D 2.16±0.01 nM) and LexAΔ24aa (K_D 4.94±0.03 nM) was within two-fold range, while a seventeen-fold reduction with LexAΔ18aa (K_D 34.4±0.19) and no observable binding with RKG/AAA mutant was observed. Mtb LexA was found to bind different "SOS" boxes under mycobacterial "SOS" regulation with comparable affinity. Association to perfectly palindromic sequence was found to be stronger. However, since association and dissociation rates changed proportionately for all the "SOS" boxes, the overall affinities were found to fall in a close range. Although Mtb LexA binds to different "SOS" boxes with comparable affinity *in-vitro*, in the cellular context, the time and spatial regulation of "SOS" genes might be altered by other transcription factors, intracellular pH, specific cations, and anions. *In-vivo* studies may uncover their actual regulation under DNA damaging and normal conditions. DNA binding assays under both physiological and extreme acidic pH conditions *in-vitro* revealed that mycobacterial LexA retains DNA binding even at pH as low as 4, albeit with reduced affinity as compared to its optimum binding at physiological pH. Taken together, our study provides a better understanding of the real-time

kinetics of mycobacterial “SOS” regulation. Extensive characterization of Mtb LexA in controlling one of the key stress-responsive pathways of the bacteria is imperative and will facilitate designing unconventional and yet more effective therapeutic strategies in counteracting TB infection.

Figure captions:

Figure 1. Phylogenetic analysis and domain architecture of Mtb LexA. (**A**) Phylogenetic tree of LexA protein sequence of 24 species. The protein sequences are clustered into 4 groups: Actinobacteria, Proteobacteria, Euryarchaeota, and Firmicutes that include the representatives from some of the major groups of bacteria. (**B**) Comparison of LexA sequences among tuberculous, non-tuberculous mycobacterial species and model Gram-negative organism, *E.coli*. The first 24 amino acids extension, the N-terminal DNA binding domain, linker region, the stretch of 18 amino acids insert in the linker and C-terminal dimerization domain are shown as a bar representation below the sequence in magenta, light blue, dark blue, yellow, and light green respectively. DNA binding residues chosen for mutation are shown with a brown bar representation below. Sequence alignment was done using Clustal Omega and ESPript was used to generate the figure. (**C**) Representation of constructs generated for this study is shown and the gel picture shows purified Mtb LexA and its variants resolved and visualized on 12% SDS PAGE.

Figure 2. Biochemical analysis and DNA binding property of Mtb LexA and its variants. (**A**) The secondary structure of WT Mtb LexA, LexAΔ24aa, LexAΔ18aa, and LexA RKG/AAA were compared using CD spectroscopy, monitored at wavelengths ranging from 195-280 nm. (**B**) Gel image showing glutaraldehyde cross-linking of Mtb LexA and its variants. Dimeric states of proteins are boxed. (**C-F**) Changes in extrinsic fluorescence spectra of the proteins, (**C**) WT Mtb LexA,(**D**) LexA RKG/AAA, (**E**) LexAΔ18aa, and (**F**) LexAΔ24aa, as seen when incubated at 1:2 ratios with non-biotinylated *dnaE2* "SOS" box (sequence given in **Table 1**) indicates the conformational changes of the proteins upon DNA binding. Fluorescence intensity is shown in arbitrary units.

Figure 3. DNA binding properties of Mtb LexA and its variants compared by EMSA analysis. (**A**) EMSA analysis of WT Mtb LexA binding to ^{32}P end-labeled ds 44 mer ds *dnaE2* "SOS" box containing DNA at 0, 1, 2, 4, 8, 16, 32, 64, 128 nM is shown. (**B**) 128 nM of WT, LexAΔ24aa, LexAΔ18aa, and LexA RKG/AAA were incubated with 3.5 nM of ^{32}P end-labeled ds 44 mer ds *dnaE2* "SOS" box containing DNA (sequence given in **Table 1**) and EMSA was carried out according to standardized conditions mentioned in Materials and Methods.

Figure 4. Kinetic analysis of DNA binding of Mtb LexA and its variants to *dnaE2* "SOS" box at physiological pH. Representative BLI sensograms showing the real-time concentration-dependent (each concentration depicted by a different color indicated in the box below) binding of WT Mtb LexA and its variants, LexAΔ18aa, and LexAΔ24aa to biotinylated 44 mer *dnaE2* "SOS" box at physiological pH (**A**, **B**, **C**), the kinetic parameters obtained from which are tabulated in **Table 2**. The corresponding response versus concentration curves has been plotted in (**D**, **E**, **F**) from the results of three independent experiments. (**G**) Representative BLI sensogram showing absence of binding of LexA RKG/AAA to biotinylated 44 mer *dnaE2* "SOS" box at physiological pH.

Figure 5. Kinetic analysis of DNA binding of Mtb LexA and its variants to *dnaE2* "SOS" box at acidic pH. Representative BLI sensograms showing the real-time concentration-dependent (each concentration depicted by a different color indicated in the box below) binding of WT Mtb LexA and its variants, LexAΔ18aa, and LexAΔ24aa to biotinylated 44 mer *dnaE2* "SOS" box at pH 4 (**A**, **B**, **C**), the kinetic parameters obtained from which are tabulated in **Table 2**. The corresponding response versus concentration curves has been plotted in (**D**, **E**, **F**) from the results of three independent experiments.

Figure 6. DNA binding kinetics of Mtb LexA to various "SOS" boxes. Representative BLI sensograms showing the real-time concentration-dependent (each concentration depicted by a different color indicated in the box below) binding of WT Mtb LexA to 44 mer biotinylated "SOS" boxes of (**A**) *lexA*, (**B**) *rv3074*, and (**C**) *recA*, the kinetic parameters obtained from which are tabulated in **Table 3**. **(D**) Comparison in binding by plotting association constants (Ka) of WT Mtb LexA to different "SOS" boxes from 3 independent experiments is shown. Association constants (Ka) are inverse of equilibrium dissociation constants or K_D values obtained from kinetic analyses.

Associated Content. Supplementary Material. The Supplementary Material file is available with this manuscript. It includes the following:

Supplementary Table Captions:

Table S1: Bacterial strains and plasmids.

Table S2: Oligonucleotide primers used in this study.

Table S3: Assessment of DNA binding properties of Mtb LexA variants to various "SOS" boxes: Kinetic parameters obtained from binding studies performed using BLI.

Supplementary Figure Captions:

Figure S1. Multiple sequence analysis of LexA protein. Comparison between sequences of Mtb LexA with LexA proteins from representatives from Actinobacteria, Proteobacteria, Euryarchaeota, and Firmicutes are shown. The first 24 amino acids extension, the N-terminal DBD, linker region, and CTD are represented as colored bars below the sequences in magenta, light blue, dark blue, and light green respectively. Conserved DNA binding residues

490 are shown with a brown bar representation below. Sequence alignment was done using
491 Clustal Omega and ESPript was used to generate the figure.

492 **Figure S2. Analysis of the oligomeric state of Mtb LexA and its variants.** Gel Filtration
493 analysis of (**A**) WT Mtb LexA and its variants, (**B**) RKG/AAA, (**C**) LexAΔ18aa and (**D**)
494 LexAΔ24aa. 500 µl was injected and run in Superdex 75 10/300 column pre-equilibrated
495 with 20 mM Tris-Cl, pH 7.5, 100 mM NaCl, and 5% glycerol. (**E**) Approximate molecular
496 weight of Mtb LexA and its variants plotted by comparing with standard markers.
497
498 **Figure S3. Assessment of DNA binding property of LexAΔ24aa (without N-terminal 6x**
499 **His tag).** Representative BLI sensogram showing the real-time concentration-dependent
500 (each concentration depicted by a different color indicated in the box below) binding of
501 LexAΔ24aa variant to biotinylated 44 mer lexA "SOS" box at physiological pH, the kinetic
502 parameters obtained from which are tabulated and shown in the inset (**A**). The corresponding
503 response versus concentration curve has been plotted in (**B**) from the results of three
504 independent experiments.
505
506
507 **Figure S4. Assessment of DNA binding properties of variants of Mtb LexA to various**
508 **"SOS" boxes.** BLI sensograms showing the real-time concentration-dependent (each
509 concentration depicted by a different color indicated in the box below) binding of
510 LexAΔ24aa to 44 mer biotinylated "SOS" boxes of (**A**) *lexA*, (**B**) *rv3074* and (**C**) *recA* and of
511 LexAΔ18aa to 44 mer biotinylated "SOS" boxes of (**D**) *lexA*, (**E**) *rv3074* and (**F**) *recA*,
512 respectively, the kinetic parameters obtained from which are tabulated in **Table S3**..
513
514
515 .

Acknowledgments

The authors are grateful to members of ATPC Facility, Faridabad for permitting usage of the BLI Facility, technical assistance from members of Pall Corporation, and the CD facility at IIT Kanpur. Graphical abstract was created using BioRender. MS is supported by DBT IYBA (2016). SERB (EMR/2017/004846) and STARS-MHRD (STARS/APR2019/BS/672), the Government of India is acknowledged for funding. CC acknowledges the Ministry of Human Resource Development, Government of India, for the fellowship.

Funding Statement

This project has been funded by STARS-MHRD (STARS/APR2019/BS/672) and SERB (EMR/2017/004846).

Author contributions

CC performed the experiments. CC, SM, and MS designed the experiments. SM and SD prepared constructs used in the study. DP performed bioinformatic analyses. CC wrote the original draft. CC, SM, and MS edited the manuscript. MS supervised the study.

Data availability statement

All supporting data and sequence information are included within the main article and its supplementary material.

Conflicts of interest

The authors declare no conflict of interest.

References

1. Cirz RT, Jones MB, Gingles NA, Minogue TD, Jarrahi B, Peterson SN, et al. Complete and SOS-Mediated Response of Staphylococcus aureus to the Antibiotic Ciprofloxacin. Journal of Bacteriology. 2007;189(2):531-9.
2. Beaber JW, Hochhut B, Waldor MK. SOS response promotes horizontal dissemination of antibiotic resistance genes. Nature. 2004;427(6969):72-4.
3. Boshoff HI, Reed MB, Barry CE, 3rd, Mizrahi V. DnaE2 polymerase contributes to in vivo survival and the emergence of drug resistance in Mycobacterium tuberculosis. Cell. 2003;113(2):183-93.
4. Michel B. After 30 Years of Study, the Bacterial SOS Response Still Surprises Us. PLOS Biology. 2005;3(7):e255.
5. Baharoglu Z, Mazel D. SOS, the formidable strategy of bacteria against aggressions. FEMS Microbiology Reviews. 2014;38(6):1126-45.
6. Sanchez-Alberola N, Campoy S, Barbé J, Erill I. Analysis of the SOS response of Vibrio and other bacteria with multiple chromosomes. BMC Genomics. 2012;13(1):58.
7. Maslowska KH, Makiela-Dzbenska K, Fijalkowska IJ. The SOS system: A complex and tightly regulated response to DNA damage. Environmental and Molecular Mutagenesis. 2019;60(4):368-84.
8. Erill I, Escribano M, Campoy S, Barbé J. In silico analysis reveals substantial variability in the gene contents of the gamma proteobacteria LexA-regulon. Bioinformatics. 2003;19(17):2225-36.
9. Rand L, Hinds J, Springer B, Sander P, Buxton RS, Davis EO. The majority of inducible DNA repair genes in Mycobacterium tuberculosis are induced independently of RecA. Mol Microbiol. 2003;50(3):1031-42.
10. Groban ES, Johnson MB, Banky P, Burnett PG, Calderon GL, Dwyer EC, et al. Binding of the Bacillus subtilis LexA protein to the SOS operator. Nucleic Acids Res. 2005;33(19):6287-95.
11. Patterson-Fortin LM, Owttrim GW. A Synechocystis LexA-orthologue binds direct repeats in target genes. FEBS Letters. 2008;582(16):2424-30.
12. Smollett KL, Smith KM, Kahramanoglou C, Arnvig KB, Buxton RS, Davis EO. Global analysis of the regulon of the transcriptional repressor LexA, a key component of SOS response in Mycobacterium tuberculosis. J Biol Chem. 2012;287(26):22004-14.
13. Chandran AV, Srikalaivani R, Paul A, Vijayan M. Biochemical characterization of Mycobacterium tuberculosis LexA and structural studies of its C-terminal segment. Acta Crystallogr D Struct Biol. 2019;75(Pt 1):41-55.
14. Smollett KL, Fivian-Hughes AS, Smith JE, Chang A, Rao T, Davis EO. Experimental determination of translational start sites resolves uncertainties in genomic open reading frame predictions - application to Mycobacterium tuberculosis. Microbiology (Reading, England). 2009;155(Pt 1):186-97.
15. Stamatakis A. RAxML version 8: a tool for phylogenetic analysis and post-analysis of large phylogenies. Bioinformatics. 2014;30(9):1312-3.
16. Ciccarelli FD, Doerks T, von Mering C, Creevey CJ, Snel B, Bork P. Toward automatic reconstruction of a highly resolved tree of life. Science. 2006;311(5765):1283-7.
17. Erill I, Jara M, Salvador N, Escribano M, Campoy S, Barbé J. Differences in LexA regulon structure among Proteobacteria through in vivo assisted comparative genomics. Nucleic acids research. 2004;32(22):6617-26.
18. Weinert LA, Welch JJ. Why Might Bacterial Pathogens Have Small Genomes? Trends Ecol Evol. 2017;32(12):936-47.

19. Zhang APP, Pigli YZ, Rice PA. Structure of the LexA–DNA complex and implications for SOS box measurement. Nature. 2010;466(7308):883-6.
20. Taylor IA, Kneale GG. A competition assay for DNA binding using the fluorescent probe ANS. Methods in molecular biology (Clifton, NJ). 2009;543:577-87.
21. Davis EO, Dullaghan EM, Rand L. Definition of the Mycobacterial SOS Box and Use To Identify LexA-Regulated Genes in Mycobacterium tuberculosis. Journal of Bacteriology. 2002;184(12):3287-95.
22. Rao M, Streur TL, Aldwell FE, Cook GM. Intracellular pH regulation by Mycobacterium smegmatis and Mycobacterium bovis BCG. Microbiology (Reading). 2001;147(Pt 4):1017-24.
23. Relan NK, Jenuwine ES, Gumbs OH, Shaner SL. Preferential interactions of the Escherichia coli LexA repressor with anions and protons are coupled to binding the recA operator. Biochemistry. 1997;36(5):1077-84.
24. Dri AM, Moreau PL. Control of the LexA regulon by pH: evidence for a reversible inactivation of the LexA repressor during the growth cycle of Escherichia coli. Mol Microbiol. 1994;12(4):621-9.
25. Hurstel S, Granger-Schnarr M, Daune M, Schnarr M. In vitro binding of LexA repressor to DNA: evidence for the involvement of the amino-terminal domain. EMBO J. 1986;5(4):793-8.
26. Simmons LA, Foti JJ, Cohen SE, Walker GC. The SOS Regulatory Network. EcoSal Plus. 2008;2008:10.1128/ecosalplus.5.4.3.

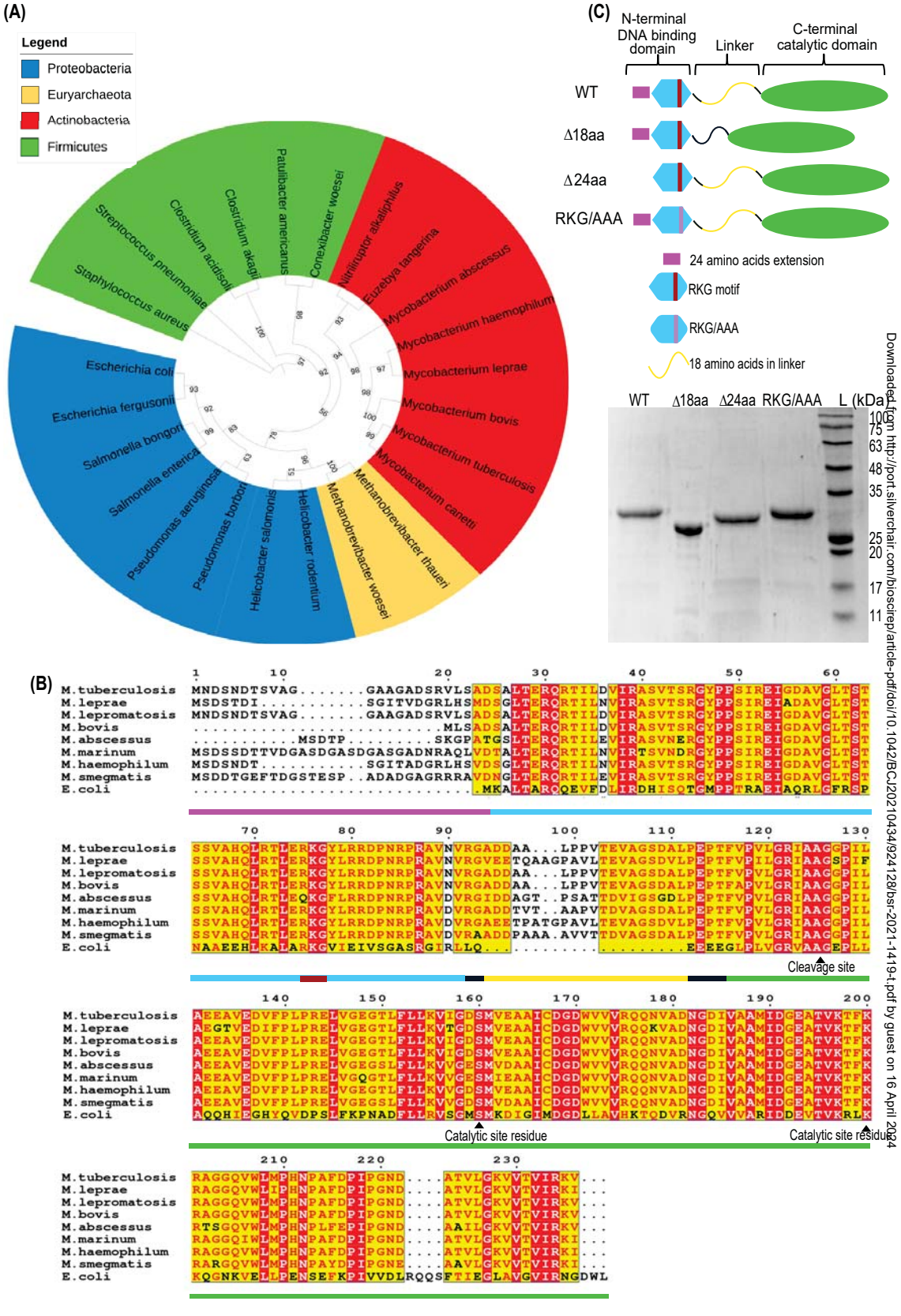

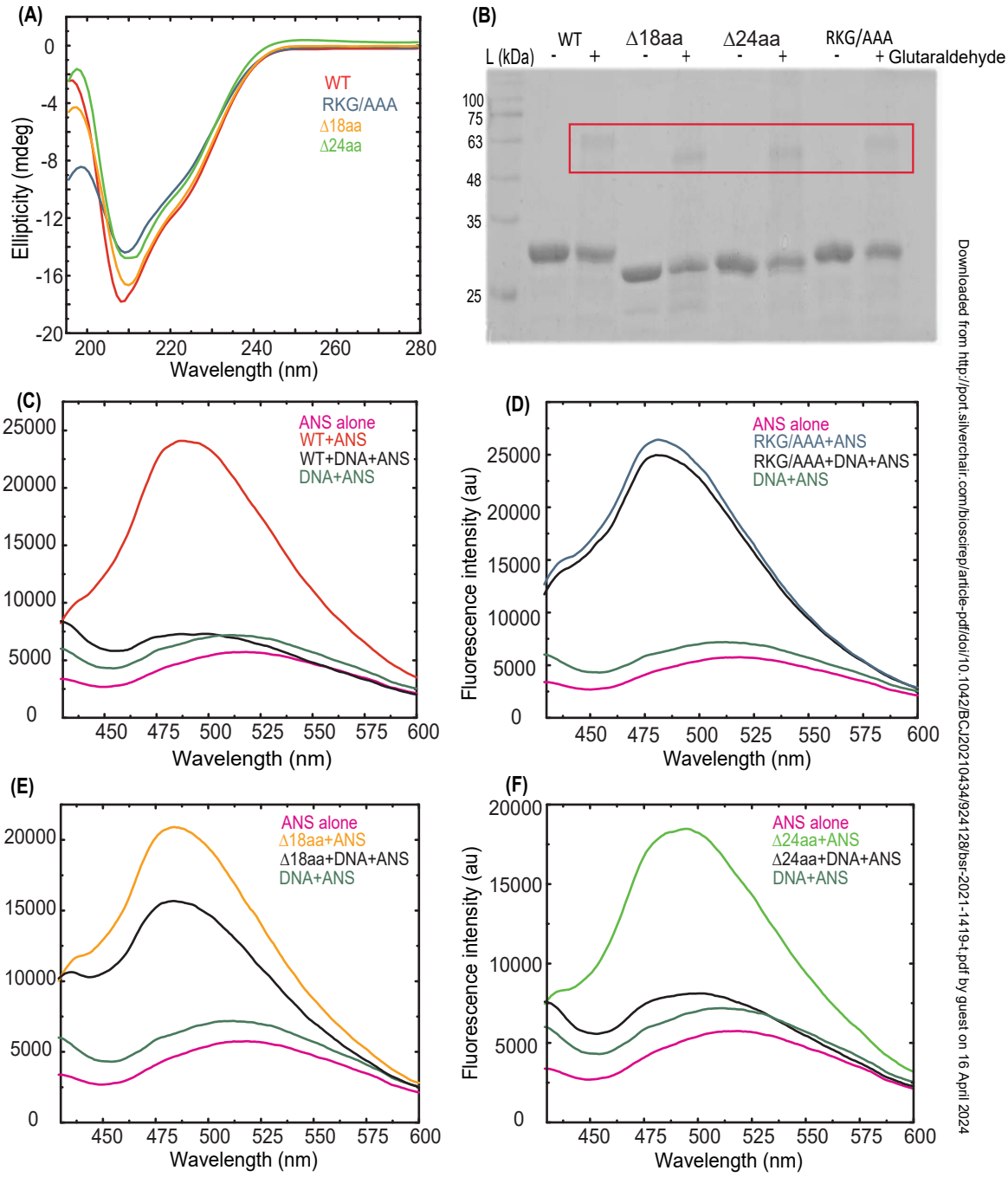

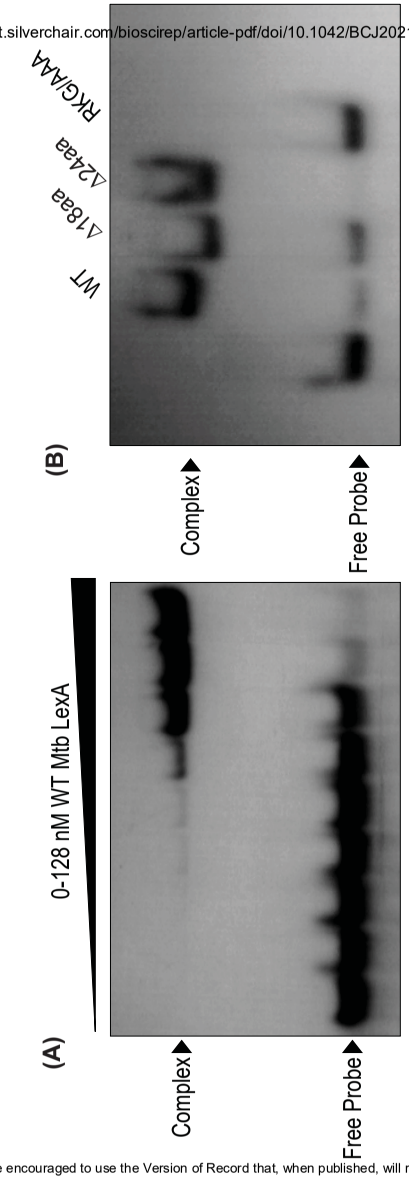

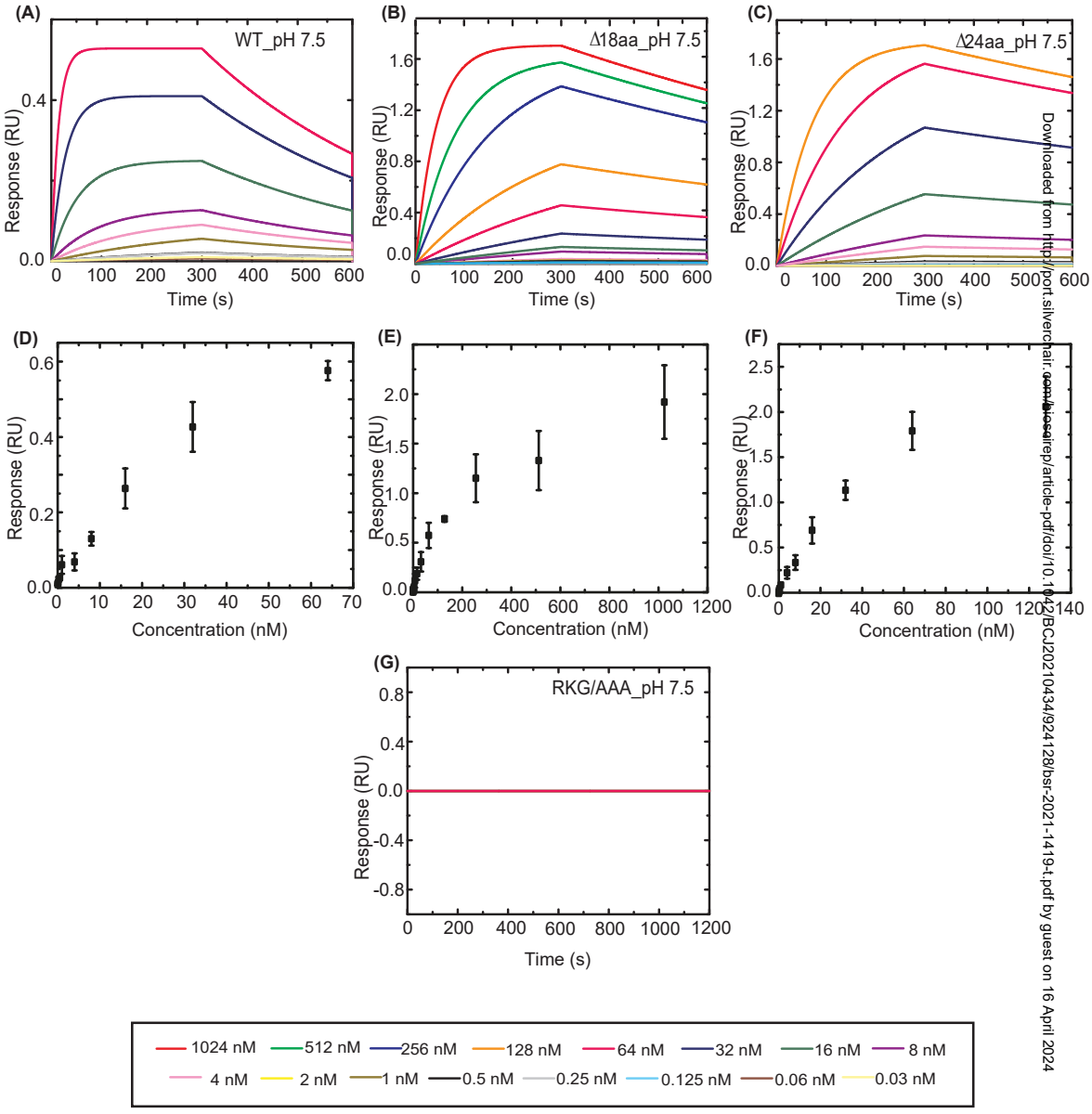

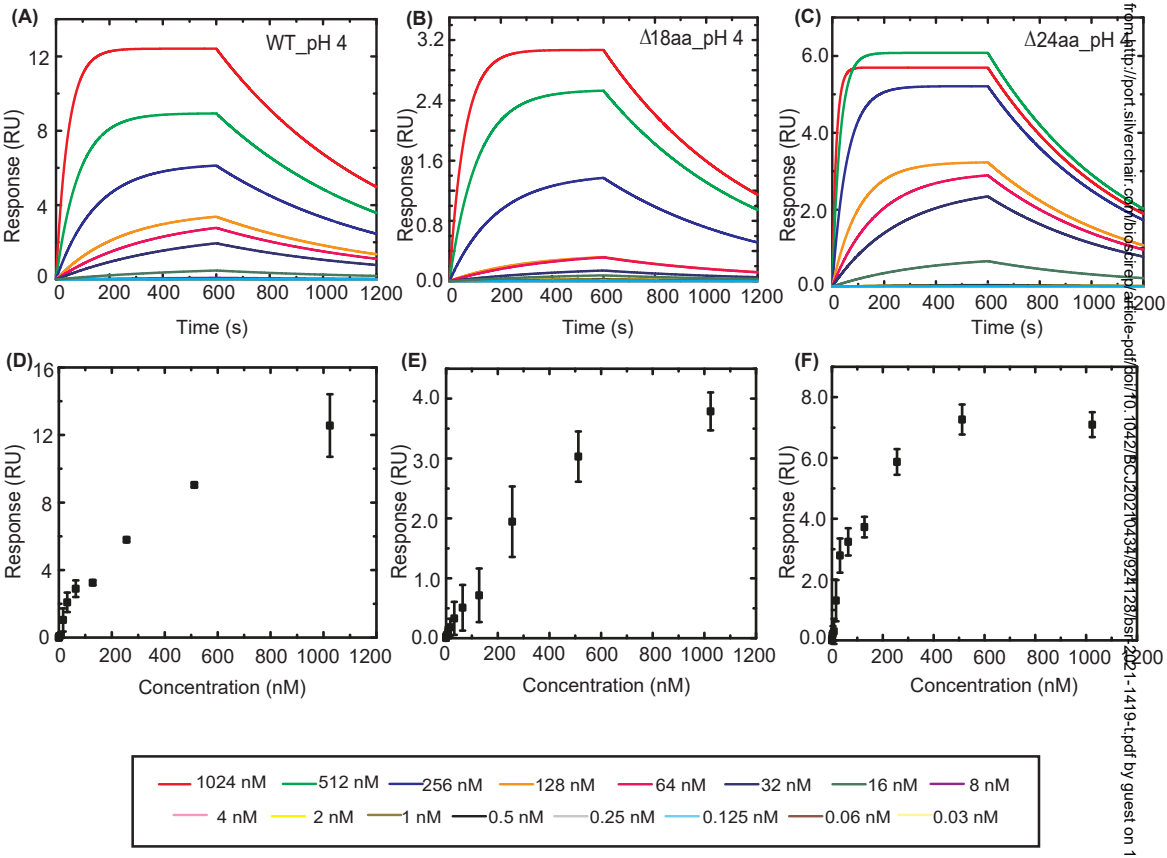

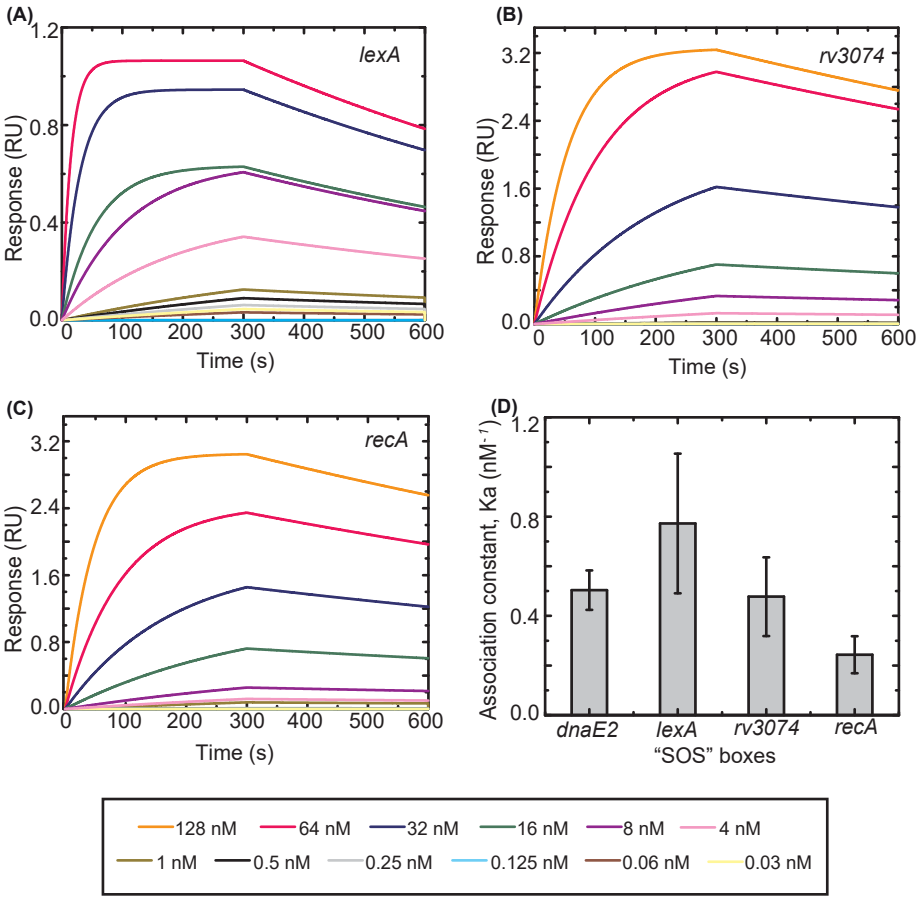

Table 1: "SOS" boxes chosen for binding studies

Duplex	Oligonucleotides used for DNA binding analysis and kinetics*
*dnaE2*_44mer	FP- 5′ Btn[#]-ACAACTGCGCTGTA**TCGAAC**<u>**AATT**</u>**GTTCGA**TATACTGTGGAATG 3′
	RP- 3′ TGTTGACGCGACAT**AGCTTG**<u>**TTAA**</u>**CAAGCT**ATATGACACCTTAC 5′
	(Perfect palindrome)
*lexA*_44mer	FP- 5′ Btn-CCGGAACACGCCTG**TCGAAC**<u>**ACAT**</u>**GTTTGA**TTCTTGGTGCGAAT 3′
	RP- 3′ GGCCTTGTGCGGAC**AGCTTG**<u>**TGTA**</u>**CAAACT**AAGAACCACGCTTA 5′
	(**Imperfect** palindrome)
*recA*_44mer	FP- 5′ Btn-GTGTCACACTTGAA**TCGAAC**<u>**AGGT**</u>**GTTCGG**CTACTGTGGTGATC 3′
	RP- 3′ CACAGTGTGAACTT**AGCTTG**<u>**TCCA**</u>**CAAGCC**GATGACACCACTAG 5′
	(**Imperfect** palindrome)
*rv3074*_44mer	FP- 5′ Btn-GCAGGCTGCTATTC**TCGAAC**<u>**ACAT**</u>**GTTCGA**GACATTGACCGCGA 3′
	RP- 3′ CGTCCGACGATAAG**AGCTTG**<u>**TGTA**</u>**CAAGCT**CTGTAACTGGCGCT 5′
	(Perfect palindrome on the repeat flanks, not in the sequences <u>**in between**</u>)

*"SOS" box sequences are highlighted in **bold**

[#]Btn stands for biotinylation

Table 2: Kinetic parameters obtained from binding studies performed using BLI.

Protein	k_{on} ($M^{-1}s^{-1}$) x 10^5	k_{off} (1/s) (s^{-1}) x 10^{-3}	K_D (nM)	R^2
LexA (pH 7.5)	10.55±0.06	2.28±0.007	2.16±0.01	0.99
LexAΔ18aa (pH 7.5)	0.22±0.0007	0.76±0.004	34.4±0.19	0.99
LexAΔ24aa (pH 7.5)	1.06±0.003	0.52±0.003	4.94±0.03	0.99
LexA (pH 4)	0.20±0.0006	1.52±0.002	75.99±0.27	0.99
LexAΔ18aa (pH 4)	0.15±0.0004	1.64±0.002	111±0.33	0.99
LexAΔ24aa (pH 4)	0.61±0.003	1.84±0.003	29.94±0.13	0.98

Table 3: Kinetic parameters obtained from binding studies of WT Mtb LexA with various "SOS" boxes performed using BLI.

"SOS" boxes	k_{on} $(M^{-1}s^{-1}) \times 10^5$	k_{off} $(s^{-1}) \times 10^{-3}$	K_D (nM)	R^2
dnaE2	10.55±0.06	2.28±0.007	2.16±0.01	0.99
lexA	10.27±0.04	1.01±0.004	0.98±0.01	0.99
rv3074	1.39±0.004	0.53±0.004	3.86±0.03	0.99
recA	1.61±0.005	0.59±0.004	3.63±0.02	0.99

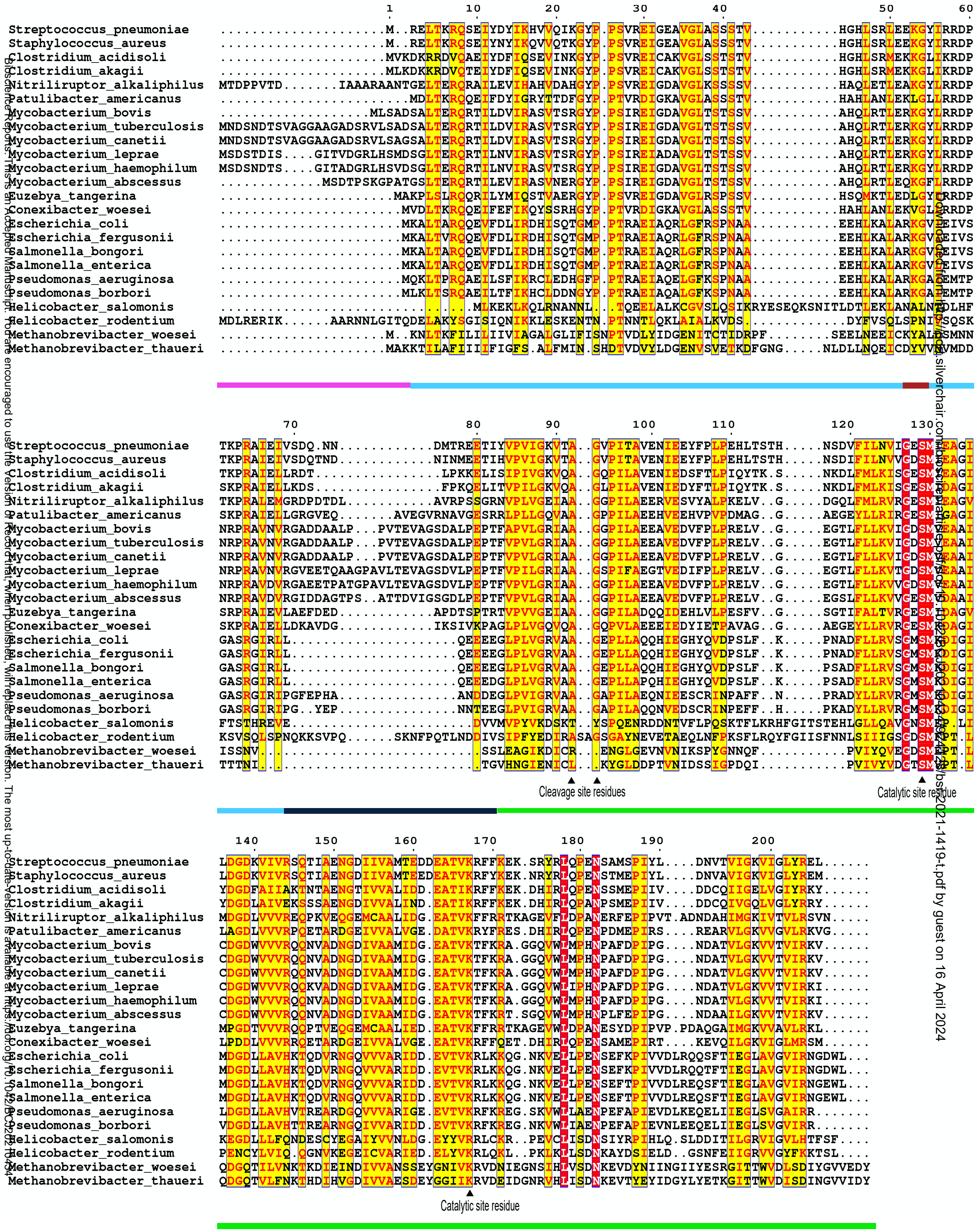

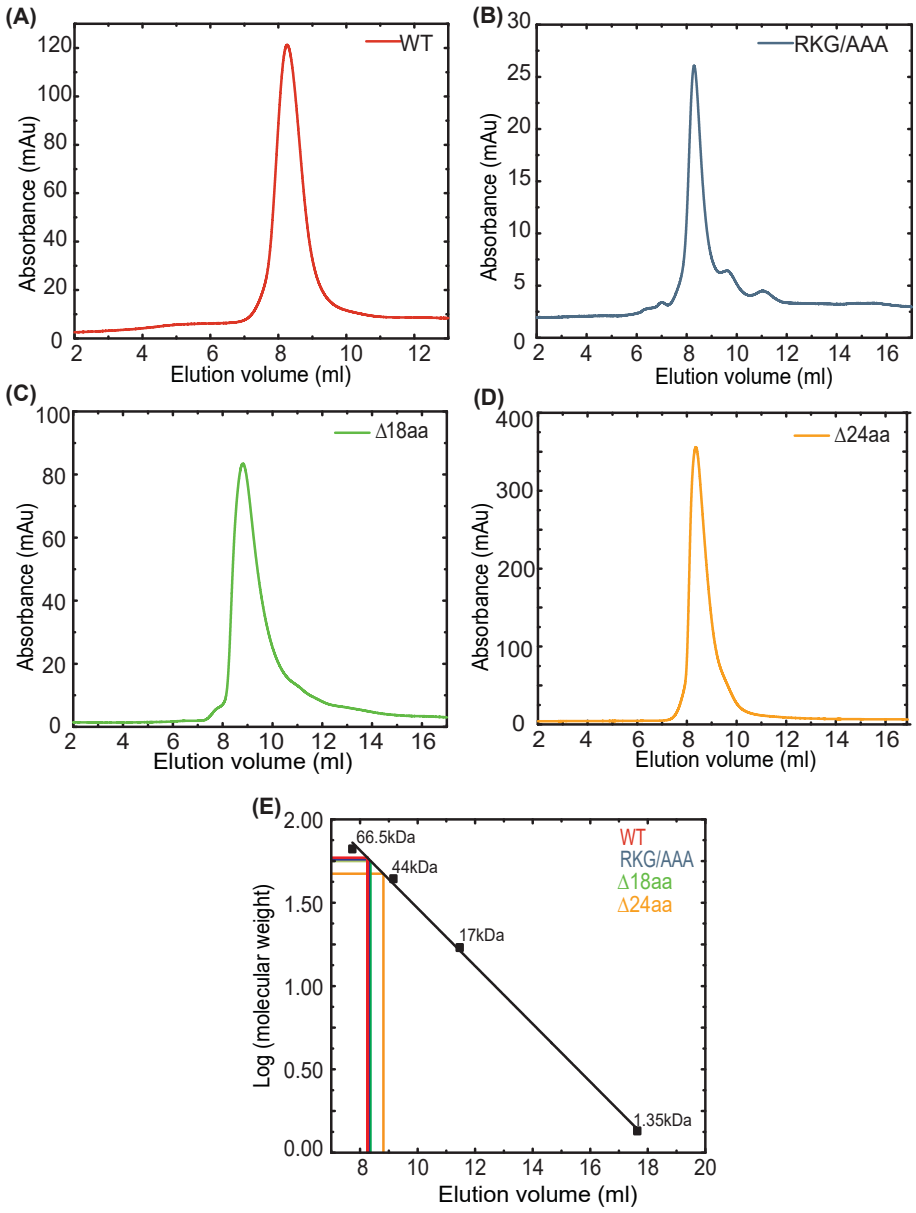

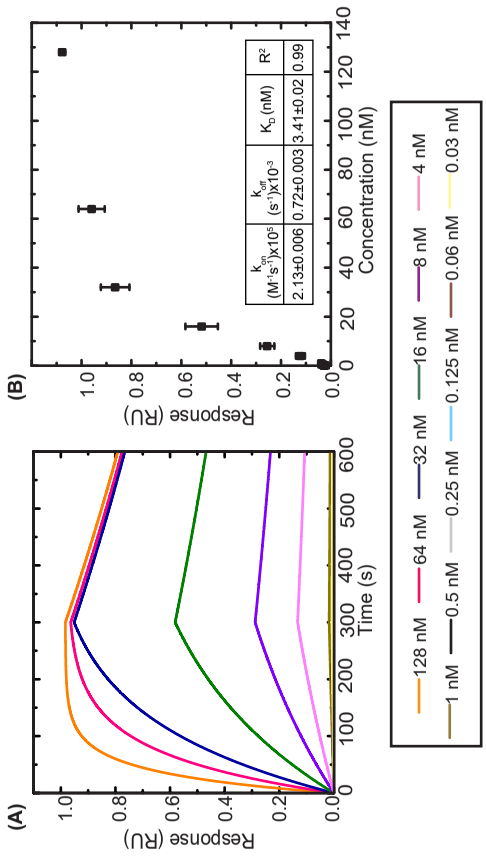

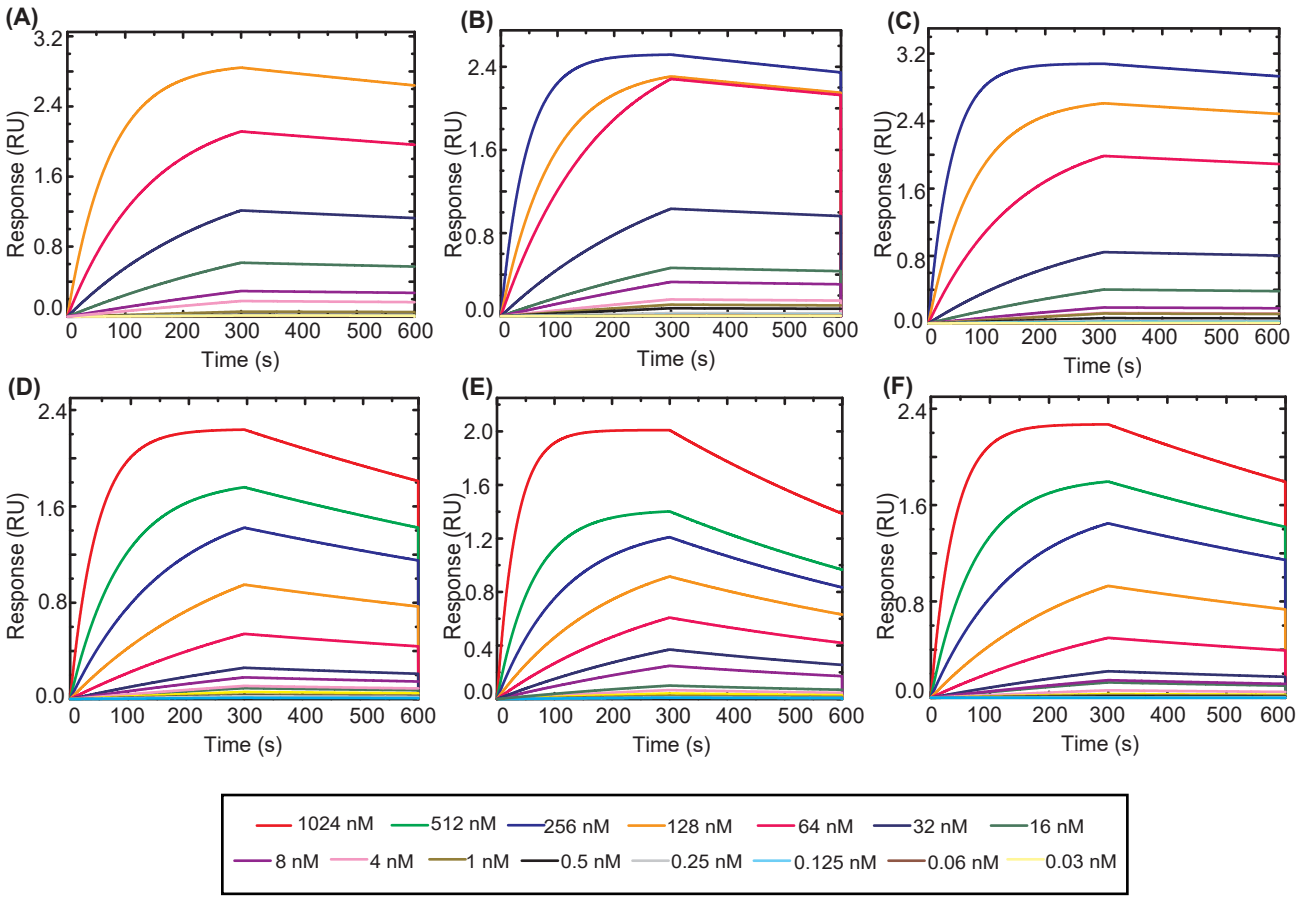

Table S1: Bacterial strains and plasmids

Name	Characteristics	Source
Bacterial Strains		
E.coli DH5α	F– φ80lacZΔ M15 Δ (*lacZYA-argF*) *U169 recA1 endA1 hsdR17* (rK– mK+) *phoA supE44* λ- *thi–1 gyrA96 relA1*	Laboratory stock
E.coli BL21(DE3)	F– *omp*T *hsdSB* (rB–, mB–) *gal dcm* (DE3)	Laboratory stock
Plasmids		
pET28a(+)	Expression vector for low copy number (pBR322 ori), strong phage promoter (T7), IPTG induction (lac operon), and Kanamycin selection (Kan^r)	Novagen
pET22b(+)	Expression vector (pBR322 ori), strong phage promoter (T7), IPTG induction (lac operon), and Ampicillin selection (Amp^r)	Novagen

Table S2: Oligonucleotide primers used in this study

Construct/Mutant	Forward Primer (FP) / Reverse Primer (RP) Sequences with restriction sites and base changes for mutation highlighted in bold
WT Mtb LexA	FP- 5′ ATGCCG **CATATG** ATGAACGACAGCAACGAC 3′
	RP- 5′ ATGCCG **GGATCC** TCAGACCTTGCGGATCAC 3′
Mtb LexAΔ18aa	FP- 5′ GTCAATGTGCGCGGTCCGGAACCCACCTTT 3′
	RP- 5′ AAAGGTGGGTTCCGGACCGCGCACATTGAC 3′
Mtb LexAΔ24aa	FP- 5′ ATAT **CATATG** TCGGCGCTGACCGAGCGGCAA 3′
	RP- 5′ ATGCCG **GGATCC** TCAGACCTTGCGGATCAC 3′
	RP- 5′ CCC **AAGCTT** GACCTTGCGGATCACCGT 3′
Mtb LexA RKG/AAA	FP- 5′ CTGCGCACCCTGGAG**GCGGCGGCG**TACCTACGCCGTGAC 3′
	RP- 5′ TCACGGCGTAGGTACGCCGCCGCCTCCAGGGTGCGCAG 3′

Table S3: Assessment of DNA binding properties of Mtb LexA variants to various "SOS" boxes: Kinetic parameters obtained from binding studies performed using BLI.

Protein	"SOS" boxes	k_{on} ($M^{-1}s^{-1}$) x 10^5	k_{off} (s^{-1}) x 10^{-3}	K_D (nM)	R^2
Mtb LexAΔ18aa	*dnaE2*	0.22±0.0007	0.76±0.004	34.40±0.19	0.99
	lexA	0.21±0.0008	0.71±0.004	34.53±0.25	0.99
	rv3074	0.28±0.0011	1.24±0.005	43.50±0.24	0.99
	recA	0.24±0.0009	0.79±0.004	32.55±0.22	0.99
Mtb LexAΔ24aa	*dnaE2*	1.06±0.003	0.52±0.003	4.94±0.03	0.99
	lexA	1.05±0.002	0.25±0.002	2.36±0.02	0.99
	rv3074	0.85±0.002	0.24±0.003	2.75±0.04	0.99
	recA	0.99±0.002	0.17±0.002	1.67±0.02	0.99